


ORIGINAL ARTICLE

Programmed death ligand-1 regulates angiogenesis and metastasis by participating in the c-JUN/VEGFR2 signaling axis in ovarian cancer

Yufei Yang^{1,5,*} | Lingfang Xia^{1,5,*} | Yong Wu^{1,*} | Hongyu Zhou^{1,5} | Xin Chen² | Haoran Li^{1,5} | Midie Xu^{4,5} | Zihao Qi⁶ | Ziliang Wang^{1,2,3}  | Huizhen Sun² | Xi Cheng^{1,5}

¹ Department of Gynecological Oncology and Cancer Research Institute, Fudan University Shanghai Cancer Center, Shanghai 200032, P. R. China

² Department of Gynecology and Obstetrics, Xinhua Hospital Affiliated to Shanghai Jiaotong University School of Medicine, Shanghai 200092, P. R. China

³ Clinical Research Unit of Shanghai Municipal Hospital of Traditional Chinese Medicine, Shanghai University of Traditional Chinese Medicine Shanghai 200071, P. R. China

⁴ Department of Pathology and Tissue Bank, Fudan University Shanghai Cancer Center, Shanghai 200032, P. R. China

⁵ Department of Oncology, Shanghai Medical College, Fudan University, Shanghai 200032, P. R. China

⁶ Department of General Surgery, Huadong Hospital Affiliated to Fudan University, Shanghai 200040, P. R. China

Correspondence

Ziliang Wang, Clinical Research Unit of Shanghai municipal Hospital of Traditional Chinese Medicine, Shanghai University of Traditional Chinese Medicine, 274 Zhijiang Middle Road, Shanghai, 200071, P. R. China.
 Email: wangziliang@xinhumed.com.cn and huf_zlwang@126.com

Xi Cheng, Department of Gynecological Oncology, Fudan University Shanghai Cancer Center; Department of Oncology, Shanghai Medical College, Fudan University, 270 Dong'an Road, Shanghai, 200032, P. R. China.
 Email: xicheng@shca.org.cn

Huizhen Sun, Department of Gynecology and Obstetrics, Xinhua Hospital Affiliated to Shanghai Jiaotong University School of Medicine, Shanghai 200092, P. R. China.
 Email: sunhuizhen@xinhumed.com.cn

Abstract

Background: Although programmed cell death-ligand 1 (PD-L1) plays a well-known function in immune checkpoint response by interacting with programmed cell death-1 (PD-1), the cell-intrinsic role of PD-L1 in tumors is still unclear. Here, we explored the molecular regulatory mechanism of PD-L1 in the progression and metastasis of ovarian cancer.

Methods: Immunohistochemistry of benign tissues and ovarian cancer samples was performed, followed by migration, invasion, and angiogenesis assays in PD-L1-knockdown ovarian cancer cells. Immunoprecipitation, mass spectrometry, and chromatin immunoprecipitation were conducted along with zebrafish and mouse experiments to explore the specific functions and mechanisms of PD-L1 in ovarian cancer.

Results: Our results showed that PD-L1 induced angiogenesis, which further promoted cell migration and invasion *in vitro* and *in vivo* of ovarian cancer. Mechanistically, PD-L1 was identified to directly interact with vascular endothelial growth factor receptor-2 (VEGFR2) and then activated the FAK/AKT pathway, which further induced angiogenesis and tumor progression, leading to poor prognosis of ovarian cancer patients. Meanwhile, PD-L1 was found to be regulated by the oncogenic transcription factor c-JUN at the transcriptional level,

This is an open access article under the terms of the [Creative Commons Attribution-NonCommercial-NoDerivs](https://creativecommons.org/licenses/by-nc-nd/4.0/) License, which permits use and distribution in any medium, provided the original work is properly cited, the use is non-commercial and no modifications or adaptations are made.

© 2021 The Authors. *Cancer Communications* published by John Wiley & Sons Australia, Ltd. on behalf of Sun Yat-sen University Cancer Center

*These authors contributed equally to this work.

which enhanced the expression of PD-L1 in ovarian cancer. Furthermore, we demonstrated that PD-L1 inhibitor durvalumab, combined with the antiangiogenic drug, apatinib, could enhance the effect of anti-angiogenesis and the inhibition of cell migration and invasion.

Conclusion: Our results demonstrated that PD-L1 promoted the angiogenesis and metastasis of ovarian cancer by participating in the c-JUN/VEGFR2 signaling axis, suggesting that the combination of PD-L1 inhibitor and antiangiogenic drugs may be considered as a potential therapeutic approach for ovarian cancer patients.

KEYWORDS

Angiogenesis, Apatinib, c-JUN, Metastasis, Ovarian Cancer, PD-L1, VEGFR2, Zebrafish

1 | BACKGROUND

Epithelial ovarian cancer is a prevalent gynecologic malignancy and is the fifth leading cause of cancer-related death in women worldwide, attributing to nearly 22,530 new cases and 13,980 deaths annually [1, 2]. Surgery and chemotherapy with platinum have been considered as the standard therapy for decades, although metastasis and recurrence rates remain high [3]. Chemotherapy resistance is also closely associated with disease progression and poor prognosis. Thus, it is increasingly urgent to identify the potential therapeutic target and develop a new therapy with improved response rates.

In the past decades, tumor angiogenesis has been proven to induce tumor progression and metastasis, and anti-angiogenic drugs may be regarded as a treatment option for patients with ovarian cancer [4, 5]. Bevacizumab, an antibody targeting the vascular endothelial growth factor (VEGF), has shown promising anti-angiogenic activity in epithelial ovarian cancer [6]. Randomized phase III trials have shown that bevacizumab plus platinum-based chemotherapy for women with advanced and recurrent disease had higher response rates and improved progression-free survival (PFS) compared with platinum-based chemotherapy alone [7–11]. The Food and Drug Administration (FDA) of USA has approved bevacizumab with or without chemotherapy as treatment in women with platinum-resistant, advanced epithelial ovarian cancer or platinum-sensitive, recurrent disease. Apatinib, a novel receptor tyrosine kinase inhibitor, was shown to target the vascular endothelial growth factor receptor-2 (VEGFR2) and was associated with improved survival of advanced ovarian cancer patients in some retrospective studies [12, 13]. Despite the efficient response to bevacizumab and apatinib, drug resistance still occurs after a few therapeutic courses. Hence, more effective treat-

ments for advanced and recurrent ovarian cancer should be urgently sought.

Programmed cell death-ligand 1 (PD-L1) was initially discovered to be upregulated in a murine T-cell hybridoma and a hematopoietic progenitor cell line [14] and interacts with programmed cell death-1 (PD-1) in the tumor microenvironment, which allows malignant tumor cells to escape from T lymphocytes' immune attack [14, 15]. To date, some PD-1/PD-L1 inhibitors, including ipilimumab, nivolumab, pembrolizumab, and more recently atezolizumab, have been used to treat multiple types of cancer, such as bladder cancer [16], gastrointestinal stromal tumor [17], gynecological cancer [18], and prostate cancer [19], which might improve the survival of these patients.

Growing evidence have shown that PD-L1 was highly expressed in various cancers, such as classical Hodgkin's lymphoma [20], non-small-cell lung cancer [21], BRAF inhibitor-resistant melanoma [22], and glioma [23]. Recently, more and more studies showed that PD-L1 played tumor-intrinsic roles in cancer progression and chemoresistance via participating in some oncogenic pathways. For instance, PD-L1 was demonstrated to promote the proliferation and metastasis of cervical cancer cells by activating the Integrin B4 (ITGB4)/Snail homolog 1 (SNAI1)/silent mating-type information regulation 3 homolog (SIRT3) signaling pathway [24] and promote bladder cancer progression and chemoresistance through the ITGB6/signal transducer and activator of transcription 3 (STAT3) signaling pathway [25]. Moreover, some studies demonstrated that PD-L1 promoted ovarian cancer tumorigenesis and progression [26, 27]. The above studies suggested that PD-L1 played a critical role in tumor progression, metastasis, and chemoresistance.

Despite all these findings, the vital role of PD-L1 in the regulation of angiogenesis, metastasis, and progression of

ovarian cancer cells remains elusive. To address the above question, we established PD-L1 silencing ovarian cancer cell lines to study its biological functions and explore the molecular mechanism.

2 | MATERIALS AND METHODS

2.1 | Patients and tissue samples

Ovarian cancer tissues were obtained from patients diagnosed between January 2008 and December 2012 at the Fudan University Shanghai Cancer Center (FUSCC; Shanghai, China), after obtaining the participants' informed consent. Epithelial ovarian cancer samples verified by postoperative pathology were included in the study, while patients with other malignant tumors were excluded.

2.2 | Cell lines and culture

Ovarian cancer cell lines OVCA433 and HeyA8 and human umbilical vein endothelial cells (HUVECs) were cultured in Dulbecco's Modified Eagle's Medium (DMEM) containing 10% fetal bovine serum (FBS, Gibco, Life Technologies, Waltham, MA, USA). All cell lines were purchased from the American type culture collection (ATCC, Manassas, VA, USA) and cultured at 37°C with 5% CO₂ atmosphere.

2.3 | Plasmid construction and viral infection

For generating stable cell lines, we obtained lentiviruses harboring control vector, VEGFR2 overexpression vector, and specific short-hairpin RNAs (shRNAs) against PD-L1 (PD-L1-sh1/2), PD-1, or c-JUN (c-JUN-sh1/2) from the Shanghai Genechem Company (Shanghai, China). Lentiviral shRNA vectors were constructed by cloning shRNA fragments into pSIH-H1-Puro (System Biosciences, San Francisco, CA, USA), and lentiviral vectors for gene overexpression were obtained via inserting PCR-amplified gene fragments into pCDH (System Biosciences).

2.4 | Reagents

PD-L1 inhibitor (durvalumab) and VEGFR2 inhibitor (apatinib) were obtained from Selleck Chemicals (Houston, TX, USA). OVCA433 and HeyA8 cells were treated with 4 μmol/L durvalumab (A2013), 20 μmol/L apatinib (S5248),

and the two-drug combination for 48 h using transwell and wound healing assays.

2.5 | Cell proliferation assay

Cell proliferation was tested by using cell counting kit 8 (CCK-8, Beyotime, Shanghai, China) following the manufacturer's instructions. Briefly, 2×10^3 cells were seeded into 96-well plates, and then 10 μL CCK-8 working solution was added to each well at different intervals. Optical density (OD) value was measured at 450 nm to determine cell proliferation.

2.6 | Wound healing assay

Cells were cultured in 6-well plates at 8×10^5 cells/well as confluent monolayers. The monolayers were wounded in a line across the middle of the well with a standard pipette tip. The wounded monolayers were subsequently washed with phosphate-buffered saline (PBS) to remove cell debris. The area of the cell-free wound was recorded with microscopy after incubating for 48 h. The images were then analyzed using the ImageJ analysis software (National Institutes of Health, Bethesda, MD, USA).

2.7 | Transwell migration/invasion assays

Transwell chambers were utilized to perform cell migration assay, and 5×10^4 cells were added into the upper chamber and the complete medium into the lower chamber. After incubating for 48 h, the cells in the upper chamber were removed using cotton swabs. The migrated cells were fixed with methanol and stained with crystal violet. Five images of different fields of view were captured for each film, and the number of migrated cells was counted. A similar insert coated with Matrigel (BD Biosciences, New York, NY, USA) was used to assess cell invasiveness in the invasion assay.

2.8 | Enzyme-linked immunosorbent assay (ELISA)

ELISA of vascular endothelial growth factor A (VEGFA) was performed using the human VEGFA-precoated ELISA Kit (SEA143Hu, Cloud-Clone Corp., Wuhan, Hubei, China). Human VEGFA-specific antibody was pre-coated in a 96-well plate. The cell supernatant and biotinylated detection antibody were added to the wells and washed once with a washing buffer. A dilution buffer (1×) was

used to dilute streptavidin-horseradish peroxidase (HRP), the mixture was added to the wells for incubation, and the HRP enzymatic reaction was visualized using 3,3',5,5'-tetramethylbenzidine (TMB) according to the manufacturer's instructions (Cloud-Clone Corp.).

2.9 | Tube formation

To further identify the effect of PD-L1 on angiogenesis, tube formation assays using HUVECs was performed. Briefly, a 300 μ L Matrigel was coated in a 24-well plate (BD Biosciences). Next, 200 μ L medium containing 2×10^4 HUVECs were layered on top of the Matrigel. HUVECs were treated with cell supernatant gained from OVCA433/PD-L1-sh1, OVCA433/PD-L1-sh2, and control cells. After 6 h of incubation, tube formation was observed under an Olympus microscope (Olympus, Tokyo, Japan).

2.10 | RNA-sequencing data analysis

Total RNA was isolated from ovarian cancer cell lines and treated with VAHTS mRNA capture beads (Vazyme, Nanjing, Jiangsu, China). Subsequent paired-end sequencing was performed with Illumina HiSeq 3000 at Ribo-Bio Co., Ltd (Guangzhou, Guangdong, China). RNA-sequencing data was analyzed by spliced read aligner HISAT2 (Dusseldorf, Germany), and gene set enrichment analysis (GSEA) was used for gene functional annotation. Genes with a fold change of > 2 and a P value of < 0.05 were considered to be significantly differentially expressed between human ovarian cancer tissues and benign tumors, OVCA433/control and OVCA433/PD-L1-sh1, or OVCA433/control and OVCA433/c-JUN-sh1 ovarian cancer cell lines.

2.11 | Immunohistochemistry assay

Paraffin-embedded tissues were incubated at 4°C overnight with the following primary antibodies: PD-L1 (ab205921, Abcam, Cambs, Britain), c-JUN (ab31419, Abcam), VEGFR2 (9698, Cell Signaling Technology, Boston, MA, USA), and VEGFA (ab52917, Abcam). Afterward, the sections were incubated with peroxidase-labeled anti-rabbit (or anti-mouse) secondary antibodies for 1 h at 37°C. Expression of proteins was semi-quantified using histochemistry score (H-score), which was calculated by the following formula: $H\text{-score} = \sum (PI \times I) = (\text{percentage of cells of weak intensity} \times 1) + (\text{percentage of cells of moderate intensity} \times 2) + (\text{percentage of cells of strong intensity} \times 3)$. According to the dyeing depth, staining

intensity of IHC was classified as negative, weak, moderate, and strong, and PI was defined as the percentage of cells with different intensity. The average H-score of the duplicate tissue microarray for each tissue type was calculated as the final score.

2.12 | Western blotting assay

The expression of PD-L1, β -actin, VEGFR2, focal adhesion kinase (FAK), p-FAK(Tyr397), AKT, p-AKT (Ser473), GATA binding protein 1 (GATA-1), N-cadherin, E-cadherin, c-JUN were detected. Protein extracts were separated by 8%-12% sodium dodecyl sulphate-polyacrylamide gel electrophoresis (SDS-PAGE) and electrotransferred to a 0.2- μ m nitrocellulose membrane. After blocking for 1 h in bovine serum albumin, the membranes were incubated with primary antibodies at 4°C overnight and then washed using 1 \times Tris-buffered saline with Tween 20 (TBST). Subsequently, the membranes were incubated with HRP-conjugated secondary antibodies and washed using TBST. Finally, protein levels were measured using the Immobilon Western Chemiluminescent HRP Substrate (Millipore, Massachusetts, USA).

2.13 | Quantitative real-time PCR (qRT-PCR)

The TRIzol reagent (Invitrogen, Carlsbad, CA, USA) was used to extract total RNA from ovarian cancer cells, xenograft tumors of nude mice, or human ovarian cancer tissues, which was subsequently reversely transcribed by the miScript Reverse Transcription Kit (Qiagen, Dusseldorf, Germany). QuantiTect Probe RT-PCR (Qiagen) was performed to quantify the RNA expression level. The reaction conditions were as follows: 95°C for 30 s (initial denaturation), followed by 40 cycles of 95°C for 5 s, 55°C for 30 s and 72°C for 30 s, after which specific amplification was measured by melting curve. Each sample was tested in triplicate and glyceraldehyde 3-phosphatedehydrogenase (GAPDH) was used in parallel reactions as an internal control. Three independent experiments were performed, and $2^{-\Delta\Delta CT}$ relative quantification was used in the final analysis. The primer sequences in the study were listed in Supplementary Table S1.

2.14 | Immunofluorescence assay

Tissues or cells were fixed with 4% paraformaldehyde for 15 min, followed by 0.3% Triton X-100 treatment for 15 min and 5% goat serum for 1 h at room temperature.

Subsequently, the samples were incubated with primary antibodies and secondary antibodies, followed by staining with 4',6-diamidino-2-phenylindole (DAPI, Life Technologies). Finally, a Leica SP5 confocal fluorescence microscope (Wetzlar, Frankfurt, Germany) was used to detect the staining effect.

2.15 | Luciferase reporter assay

CRE-luciferase (pGL3 vector) was transfected into cells, and GloMax-Multi Microplate Reader (Promega, Madison, WI, USA) was used to test the luciferase activity. Renilla luciferase acted as an internal control to normalize the reporter luciferase activities.

2.16 | Chromatin immunoprecipitation (ChIP) assay

A Pierce Agarose ChIP Kit (#27177, Thermo Fisher Scientific, Waltham, MA, USA) was used for ChIP. Chromatin was mechanically sheared using sonication after OVCA433 cell precipitation was collected and crosslinked using formaldehyde. Subsequently, immunoprecipitation was carried out with 4 mL IgG (Cell Signaling Technology), 10 μ L c-JUN (ab 31419, Abcam), or 2 mL polymerase II antibodies (Imgenex, San Diego, CA, USA). Immunoprecipitated total chromatin was then reversely crosslinked and recovered using column purification. Finally, qRT-PCR was performed using the PD-L1-specific ChIP primers.

2.17 | Immunoprecipitation (IP)

IP was performed using Pierce Crosslink Immunoprecipitation Kit (Thermo Fisher Scientific) as per the manufacturer's protocol. Briefly, 10 μ g antibody was covalently crosslinked with agarose A/G beads using disuccinimidyl suberate (DSS) and incubated with 1 mg of total cell lysate overnight at 4°C. Antigen was eluted and subjected to SDS-PAGE.

2.18 | Mass spectrometry (MS)

PD-L1-VEGFR2 complex was obtained by IP with anti-PD-L1 from OVCA433 cells. Cells were lysed in IP buffer (20 mmol/L Tris at pH 8.0, 0.25 mol/L NaCl, 0.5% NP-40, 5 mmol/L ethylenediaminetetraacetic acid) and immunoprecipitated with agarose beads (Sigma-Aldrich, St. Louis, MO, USA) for 4 h at 4°C. IP buffer and eluted PD-L1 peptide were used to wash the beads. The eluted proteins were

resolved on gradient SDS-PAGE, silver-stained, and subjected to MS sequencing and data analysis. MS assay was carried out by PTM BioLab, Inc. (Hangzhou, Zhejiang, China).

2.19 | Animal tumor model and *in vivo* imaging

Our animal experiments were approved by the Ethics Committee at FUSCC. The tumor models were established upon subcutaneous or intraperitoneal injections of OVCA433 cells ($\approx 5 \times 10^6$) into 60 4-week-old female BALB/c nude mice (Department of Laboratory Animals, FUSCC). Subcutaneous tumor volumes were measured with the following formula: volume = length \times width² \times 0.52. When the average tumor volume of 100 mm³ was reached, 30 mice were intraperitoneally treated with apatinib (50 mg/kg). The tumor volume was measured every 3 days. Ultimately, the mice were euthanized, and all the tumors were dissected and weighed. The nude mice bearing intraperitoneal tumors were measured using a luminescence imaging system (Perkin Elmer, Wellesley, MA, USA).

2.20 | Zebrafish angiogenesis study

The embryos of zebrafishes were cultured in the laboratory of Xinhua Hospital. Fertilized one-cell flil-a-enhanced green fluorescent protein transgenic line embryos were injected with 4 ng of PD-L1 morpholino or VEGFR2 cDNA recombinant plasmid to assess blood vessel formation in zebrafish. At 24 h post-fertilization, embryos were dechlorinated and anesthetized with 0.016% tricaine methane-sulfonate (MS-222, Sigma-Aldrich). Each zebrafish embryo was then placed on the lateral side and mounted with 3% methylcellulose on a depression slide for examination by fluorescence microscopy. VEGFA expression was determined by qRT-PCR. Total RNA was extracted from 15 to 20 embryos per group with TRIzol reagent (Roche, Basel, Switzerland) and reversely transcribed using the PrimeScript RT (Takara, West Tokyo, Tokyo Metropolis, Japan).

2.21 | Statistical analysis

The data were analyzed using SPSS (Version 24.0, Chicago, IL, USA) and GraphPad Prism (Version 8.0, San Diego, CA, USA) and presented as mean \pm standard deviation (SD). For comparisons between two groups of normally distributed data, Student *t*-test was used. The Kaplan-Meier method with log-rank analysis was used to estimate

overall survival (OS) and PFS. OS was measured from the date of surgery to death of any cause or until the most recent follow-up. PFS was calculated from the date of surgery to the occurrence of progression or relapse. Variables with a *P* value of < 0.05 in the univariate analysis were included in the subsequent multivariate analysis based on the Cox proportional hazards model. A probability of less than 0.05 was considered significant.

3 | RESULTS

3.1 | Expression level of PD-L1 in ovarian cancer tissues and its relationship with prognosis of ovarian cancer

Firstly, 84 benign ovarian tumor tissues (47 cystadenomas and 37 ovarian cysts), 273 primary ovarian cancer tissues, and 218 metastatic ovarian cancer tissues in the greater omentum were collected. Clinical data of the 273 primary ovarian cancer patients are summarized in Supplementary Table S2. Immunohistochemistry demonstrated that the expression of PD-L1 in primary and metastatic ovarian cancer lesions was higher than that in benign tissues (Figure 1A-C). The rate of high PD-L1 expression in late-stage ovarian cancer tissues was significantly higher than that in early-stage cancer tissues (63.5% vs. 29.2%, Figure 1D), which was also further verified by the H-Score (Figure 1E). In addition, high expression of PD-L1 was also related with the rates of ascites, lymph metastasis, and high/moderate tumor grade (Figure 1F-H). Results of survival analysis demonstrated that high expression of PD-L1 was significantly associated with shorter OS and PFS (Figure 1I). These results indicated that PD-L1 played an important role in ovarian cancer progression, and an enhanced PD-L1 might result in the poor prognosis of ovarian cancer patients.

3.2 | The role of PD-L1 in regulating cell migration and invasion of ovarian cancer

To further explore the regulatory function of PD-L1 in ovarian cancer, we introduced two PD-L1-targeting shRNAs and the control vector into ovarian cancer cell lines (PD-L1-silencing cell lines: OVCA433/PD-L1-sh1/2 and HeyA8/PD-L1-sh1/2; control cell lines: OVCA433/control and HeyA8/control), which was verified by Western blotting assay (Figure 2A). Using RNA-sequencing, we discovered that a lot of important regulatory genes participating in metastasis were significantly decreased in OVCA433/PD-L1-sh1 cells than in OVCA433/control cells (Figure 2B). Next, we measured the influence of PD-L1

silencing on ovarian cancer cell metastasis (Figure 2C-H). By performing a wound healing assay, we found that the migration range was decreased by 53.6% and 47.2% in OVCA433/PD-L1-sh1 and OVCA433/PD-L1-sh2 cells, and by 61.4% and 51.5% in HeyA8/PD-L1-sh1 and HeyA8/PD-L1-sh2 cells, respectively, compared with controls (Figure 2C, 2F). The transwell migration assay showed that the number of migrated cells was reduced by 66.7% and 56.7% in OVCA433/PD-L1-sh1 and OVCA433/PD-L1-sh2 cells and by 42.5% and 42.3% in HeyA8/PD-L1-sh1 and HeyA8/PD-L1-sh2 cells, respectively, compared with controls (Figure 2D, 2G). The transwell invasion assay showed that the number of invaded cells was reduced by 69.4% and 63.3% in OVCA433/PD-L1-sh1 and OVCA433/PD-L1-sh2 cells and by 61.7% and 63.8% in HeyA8/PD-L1-sh1 and HeyA8/PD-L1-sh2 cells, respectively, compared with controls (Figure 2E, 2H).

In addition, we tested the effect of PD-L1 silencing on ovarian cancer proliferation by cell counting kit-8 (CCK8) assay and found that PD-L1 silencing reduced cell growth significantly (Supplementary Figure S1A-B). Moreover, we added soluble PD-L1 protein to cell culture supernatant, and found no change in ovarian cancer cell metastasis (Supplementary Figure S1C-E). Therefore, we concluded that the function of PD-L1 in inducing ovarian cancer metastasis was exerted by membrane PD-L1.

Because of the importance of the PD-L1/PD-1 axis in cancer progression, we further examined the PD-1 expression in ovarian cancer cell lines, and discovered that PD-1 was lowly expressed in most ovarian cancer cells (Supplementary Figure S1F). Then, we chose the HeyA8 cell line with relatively high PD-1 expression to investigate the function of PD-1 silencing in cell growth and metastasis. The results demonstrated that there were no significant changes in these cell biological behaviors (Supplementary Figure S1G-K), excluding the possibility of PD-1 in regulating the migration and invasion of ovarian cancer cells.

3.3 | PD-L1 induces tumor angiogenesis and metastasis via VEGFR2-dependent signaling in ovarian cancer cells

The results of the ChIP assay also indicated that the genes involved in angiogenesis were slightly decreased in OVCA433/PD-L1-sh1 cells as compared with control cells (Figure 3A). To further identify the effect of PD-L1 on angiogenesis, we performed tube formation assays using HUVECs. HUVECs were treated with cell supernatant gained from OVCA433/PD-L1-sh1, OVCA433/PD-L1-sh2, and control cells. The tube formation of HUVECs in PD-L1-knockdown groups were significantly inhibited (Figure 3B-C). Reduction of VEGFA was also found in

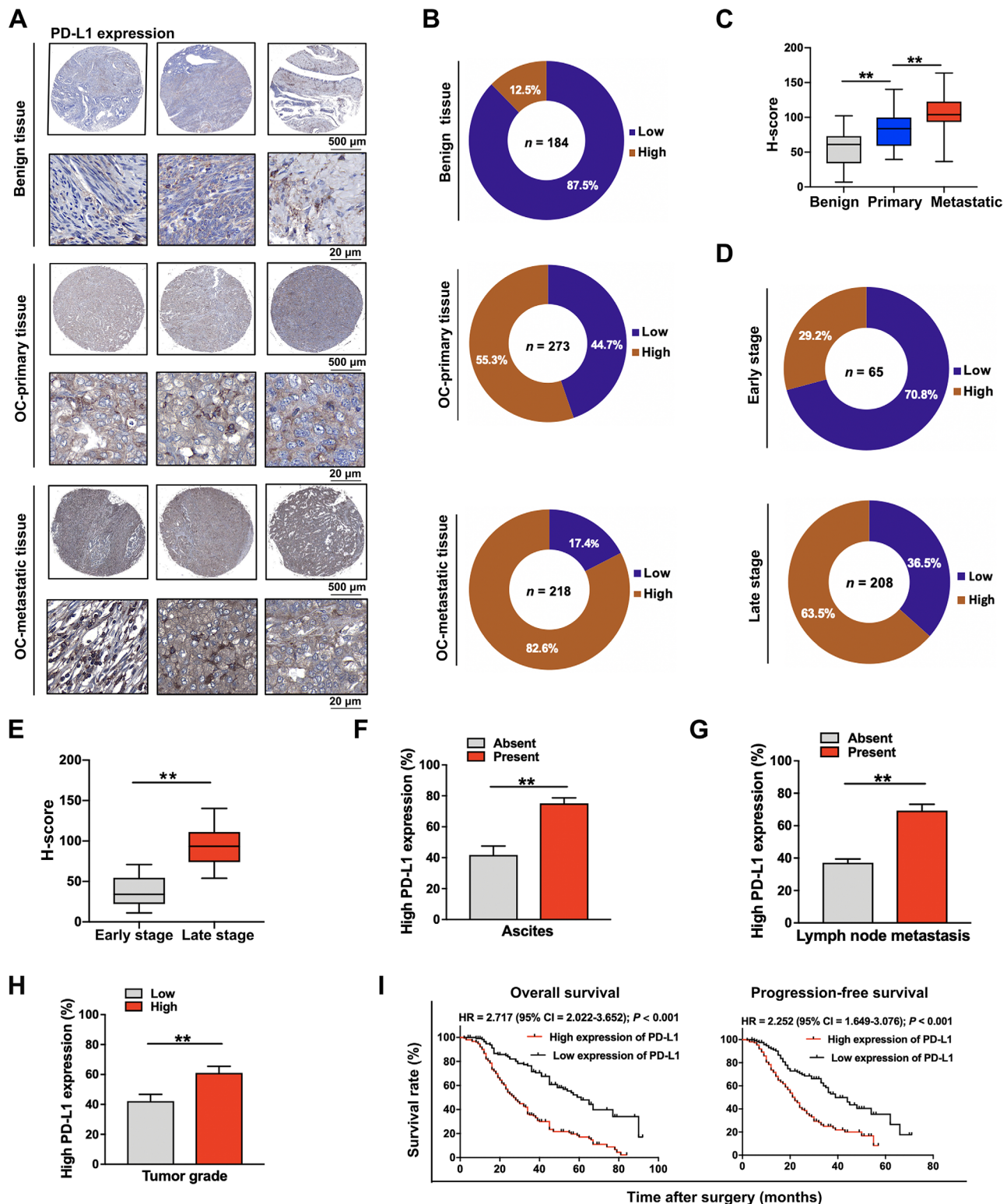


FIGURE 1 Immunohistochemical staining of PD-L1 and the survival analysis. (A–C) Immunohistochemical staining of PD-L1 in benign tumor tissues, primary ovarian cancer lesions, and metastatic ovarian cancer lesions (A: representative images; B: statistical results; C: H-score). (D) and (E) Immunohistochemical staining of PD-L1 in early- and late-stage ovarian cancer tissues (D: statistical results; E: H-score). (F) High PD-L1 expression rate in ovarian cancer tissues with or without ascites. (G) High PD-L1 expression rate in ovarian cancer tissues with or without lymph node metastasis. (H) High PD-L1 expression rate in high/moderate- and low-grade ovarian cancer tissues. (I) Overall survival and progression-free survival of ovarian cancer patients with high or low expression of PD-L1. **, $P < 0.01$. Abbreviations: PD-L1: programmed cell death-ligand 1; OC: ovarian cancer; H-score: histochemistry score; HR: hazard ratio; CI: confidence interval

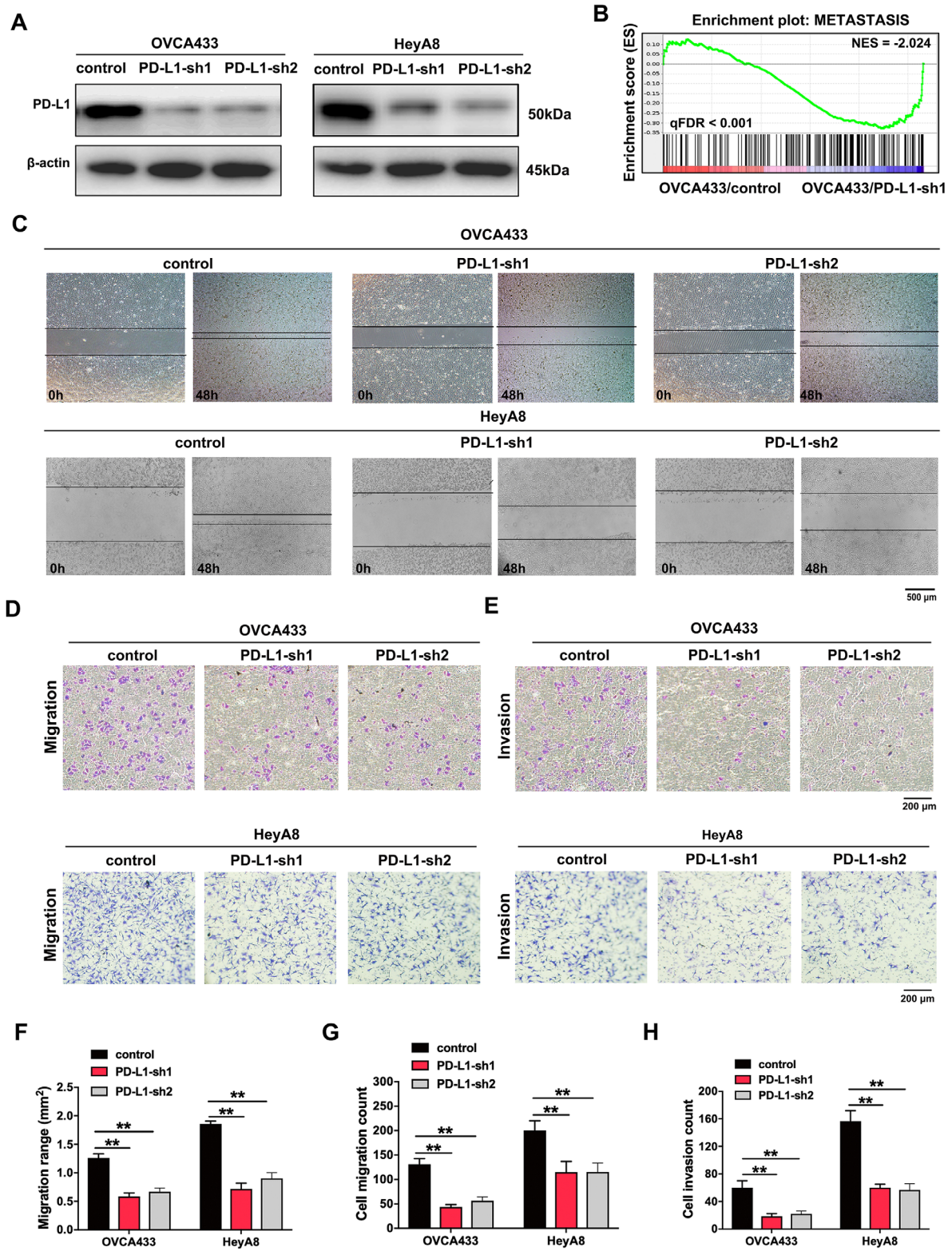
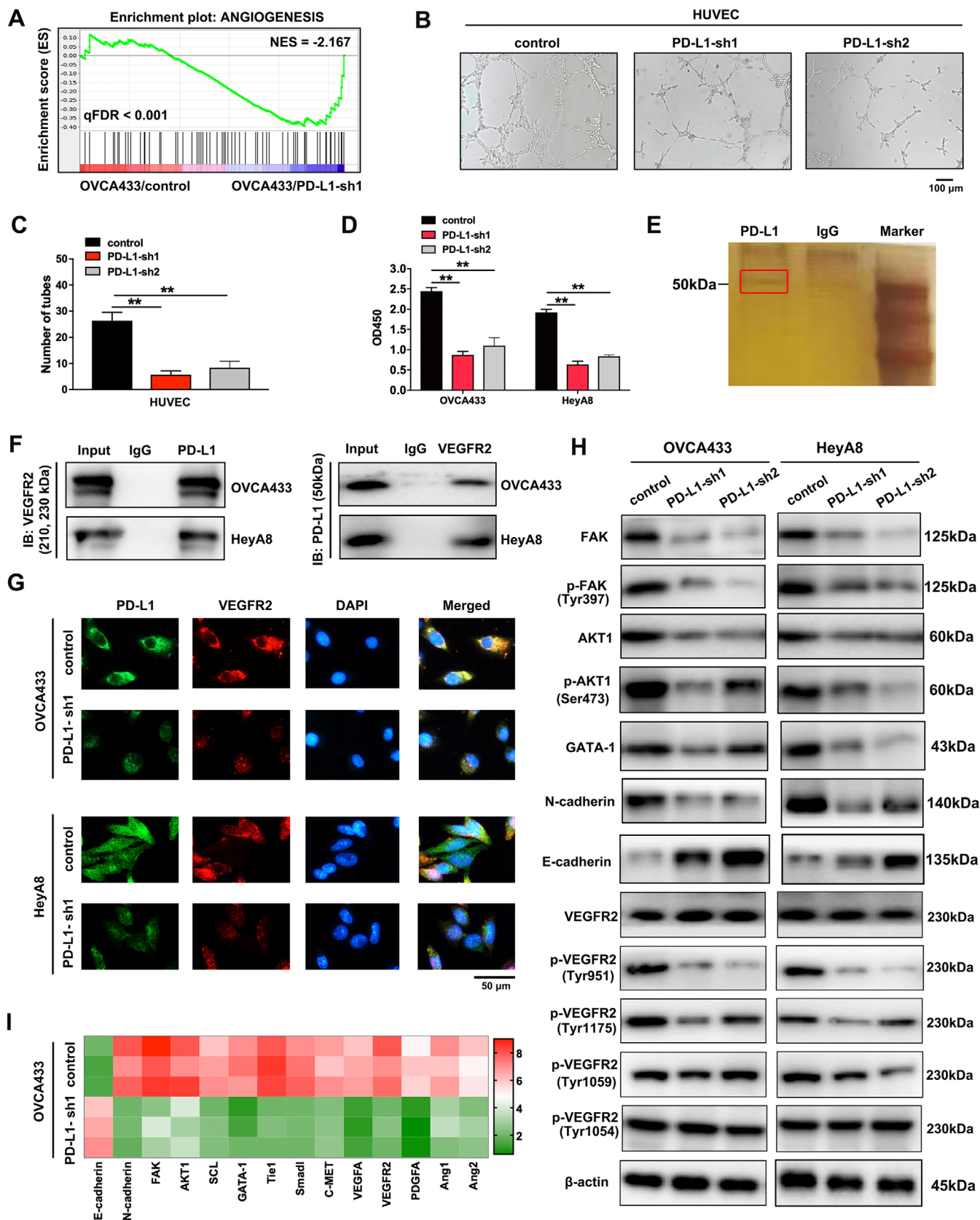


FIGURE 2 PD-L1 promotes ovarian cancer cell migration and invasion. (A) The efficiency of PD-L1 knockdown in ovarian cancer cell lines was detected by Western blotting. (B) GSEA analysis was performed using PD-L1-knockdown and control cells (OVCA433/PD-L1-sh1 and OVCA433/control). A gene signature was defined as a gene with significant expression changes. (C) Representative images of cell migration tested by wound healing assay. (D) Representative images of cell migration tested by transwell assay. (E) Representative images of cell invasion tested by transwell assay. (F-H) Quantification of cell migration and invasion tested by wound healing or transwell assays. **, $P < 0.01$. Abbreviations: PD-L1: programmed cell death-ligand 1; PD-L1-sh1/2: PD-L1 short hairpin RNA 1/2; GSEA: gene set enrichment analysis; ES: enrichment score; NES: normalized enrichment score; FDR: false discovery rate



the supernatant of PD-L1-silenced ovarian cancer cells compared with control cells by ELISA (Figure 3D). To probe into the potential targets of PD-L1, we performed IP assay and MS analyses, and found that angiogenesis closely related receptor VEGFR2 was directly bound to PD-L1 (Figure 3E), which was confirmed by Co-IP (Figure 3F) and immunofluorescence (Figure 3G). The above results indicated that VEGFR2 was a potential receptor of PD-L1 in ovarian cancer. In the rescue experiment, we found that VEGFR2 overexpression partially reversed the inhibition of migration and invasion caused by PD-L1 silencing in ovarian cancer cells (Supplementary Figure S2). The proteins associated with cell metastasis and angiogenesis, such as FAK, p-FAK (Tyr397), AKT1, p-AKT1 (Ser473) and GATA-1, were downregulated by PD-L1 silencing (Figure 3H). Interestingly, PD-L1 knockdown significantly reduced the phosphorylation of VEGFR2 tyrosine 951 residues, which induced the changes of the downstream proteins potentially. Heatmap of the qRT-PCR results showed that the FAK/AKT pathway and other metastasis- and angiogenesis-related genes were suppressed through PD-L1 silencing (Figure 3I). Thus, the abovementioned results demonstrated that PD-L1 might promote tumor angiogenesis through the VEGFR2/FAK signaling pathway.

3.4 | Combination of durvalumab with VEGFR2 blockade enhances the therapeutic effect of anti-angiogenesis targeting drugs

Next, we detected the effects of the PD-L1 inhibitor durvalumab and/or VEGFR2 inhibitor apatinib on angiogenesis, ovarian cancer cell migration, and invasion. We found

that the tube formation of HUVECs was more significantly inhibited by a combination of durvalumab and apatinib than durvalumab or apatinib alone (Figure 4A). Similarly, the migration and invasion of ovarian cancer cells were reduced by durvalumab plus apatinib than by a single drug therapy (Figure 4B-C). Together, these results demonstrated that the use of PD-L1 inhibitor in combination with VEGFR2 blockade could enhance the therapeutic effect of anti-angiogenesis targeting drugs.

3.5 | PD-L1 as a downstream target of the oncogenic transcription factor c-JUN

To explore the reason of high PD-L1 expression in ovarian cancer, RNA-sequencing assay was performed in benign tissues and ovarian cancer tissues. C-JUN was significantly enriched in ovarian cancer tissues (Figure 5A). Subsequently, we verified that c-JUN silencing reduced ovarian cancer cell migration and invasion (Supplementary Figure S3). Moreover, PD-L1 was significantly decreased in c-JUN-knockdown OVCA433 cells (Figure 5B), which was verified by qRT-PCR, Western blotting, and immunofluorescence (Figure 5C-E). Furthermore, PD-L1 overexpression might partially reverse c-JUN knockdown-induced inhibition of cell migration and invasion (Supplementary Figure S3). Considering c-JUN is a transcription factor, we hypothesized that c-JUN may regulate the transcription of PD-L1. We performed a luciferase reporter assay to confirm the mechanistic link between c-JUN and PD-L1. The knockdown of c-JUN decreased the promoter activity PD-L1 (Figure 5F). Subsequently, by performing a ChIP assay of OVCA433 cells, we identified two binding sites located at the transcription start site upstream of the PD-L1 promoter (Figure 5G). To further validate the binding

FIGURE 3 PD-L1 combines with VEGFR2 directly and regulates angiogenesis. (A) GSEA analysis was performed using PD-L1-knockdown and control cells (OVCA433/PD-L1-sh1 and OVCA433/control). A gene signature was defined as a gene with significant expression changes. (B) and (C) Effect of PD-L1 silencing on tube formation of HUVECs. HUVECs were treated with cell supernatant gained from OVCA433/PD-L1-sh1, OVCA433/PD-L1-sh2, and control cells. (D) ELISA of VEGFA in PD-L1-knockdown ovarian cancer cells and control cells. (E) Cellular extracts from OVCA433 cells were immunopurified with anti-PD-L1 affinity columns and eluted with PD-L1 peptide. The eluates were resolved by SDS-PAGE and silver stained. IgG was the negative control. (F) Co-IP analysis demonstrates an interaction between PD-L1 and VEGFR2 in ovarian cancer cell lines. (G) Immunofluorescence assay demonstrates the relationship between PD-L1 and VEGFR2. (H) Western blotting analysis of proteins associated with cancer metastasis and angiogenesis in PD-L1-silenced ovarian cancer cells and control cells. β -actin was used as a loading control. (I) Heat map of qRT-PCR analysis of indicated genes in PD-L1-knockdown and control OVCA433 cells. $**P < 0.01$. Abbreviations: PD-L1: programmed cell death-ligand 1; VEGFR2: vascular endothelial growth factor receptor 2; GSEA: gene set enrichment analysis; PD-L1-sh1/2: PD-L1 short hairpin RNA 1/2; ES: enrichment score; NES: normalized enrichment score; FDR: false discovery rate; HUVEC: human umbilical vein endothelial cell; ELISA: enzyme-linked immunosorbent assay; VEGFA: vascular endothelial growth factor A; OD: optical density; SDS-PAGE: sodium dodecyl sulfate polyacrylamide gel electrophoresis; Co-IP: co-immunoprecipitation; DAPI: 4',6-diamidino-2-phenylindole; IB: immunoblotting; qRT-PCR: quantitative real-time polymerase chain reaction; FAK: focal adhesion kinase; AKT1: protein kinase B; SCL: stem cell leukemia; Tiel: tyrosine kinase with immunoglobulin and epidermal growth factor homology domains 1; Smad1: mothers against decapentaplegic homolog 1; C-MET: cellular-mesenchymal epithelial transition factor; PDGFA: platelet-derived growth factor A; Ang1: angiopoietin 1; Ang2: angiopoietin 2

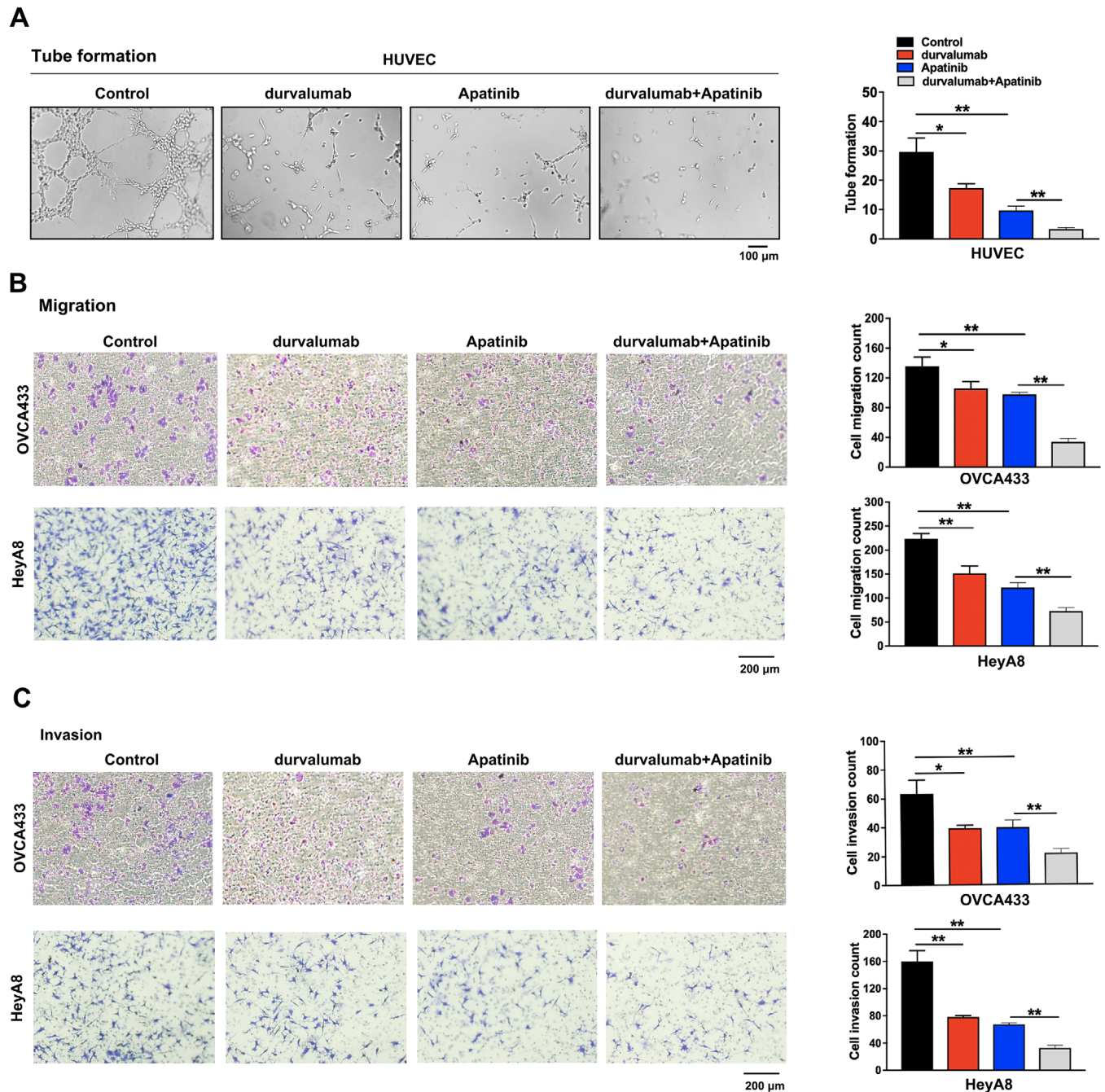


FIGURE 4 The effects of PD-L1 inhibitor durvalumab and VEGFR2 inhibitor apatinib alone or in combination on tube formation, cell migration, and invasion. (A) The effects of these treatments on tube formation. HUVECs were treated with 4 μ mol/L durvalumab and 20 μ mol/L apatinib (S5248) alone or in combination for 6 h. (B) The cell migration tested by transwell assay. OVCA433 and HeyA8 cells were treated with 4 μ mol/L durvalumab and 20 μ mol/L apatinib alone or in combination for 48 h. (C) The cell invasion tested by transwell assay. OVCA433 and HeyA8 cells were treated with the same method as above. * $P < 0.05$; ** $P < 0.01$. Abbreviations: PD-L1: programmed cell death-ligand 1; VEGFR2: vascular endothelial growth factor receptor 2; HUVEC: human umbilical vein endothelial cell

sites of c-JUN in the promoter of PD-L1, we individually mutated these two binding sites of c-JUN (Figure 5H), and both mutations efficiently abrogated the luciferase activity (Figure 5I). These results suggested that PD-L1 was a downstream target of c-JUN, and the activation of c-JUN was required for the upregulation of PD-L1 in ovarian cancer.

3.6 | PD-L1 promotes the angiogenesis and progression of ovarian cancer *in vivo*

To confirm the *in vitro* experimental results described above, we established ovarian cancer cell-derived subcutaneous and intraperitoneal xenograft models. Results of both models showed that tumor growth was significantly suppressed

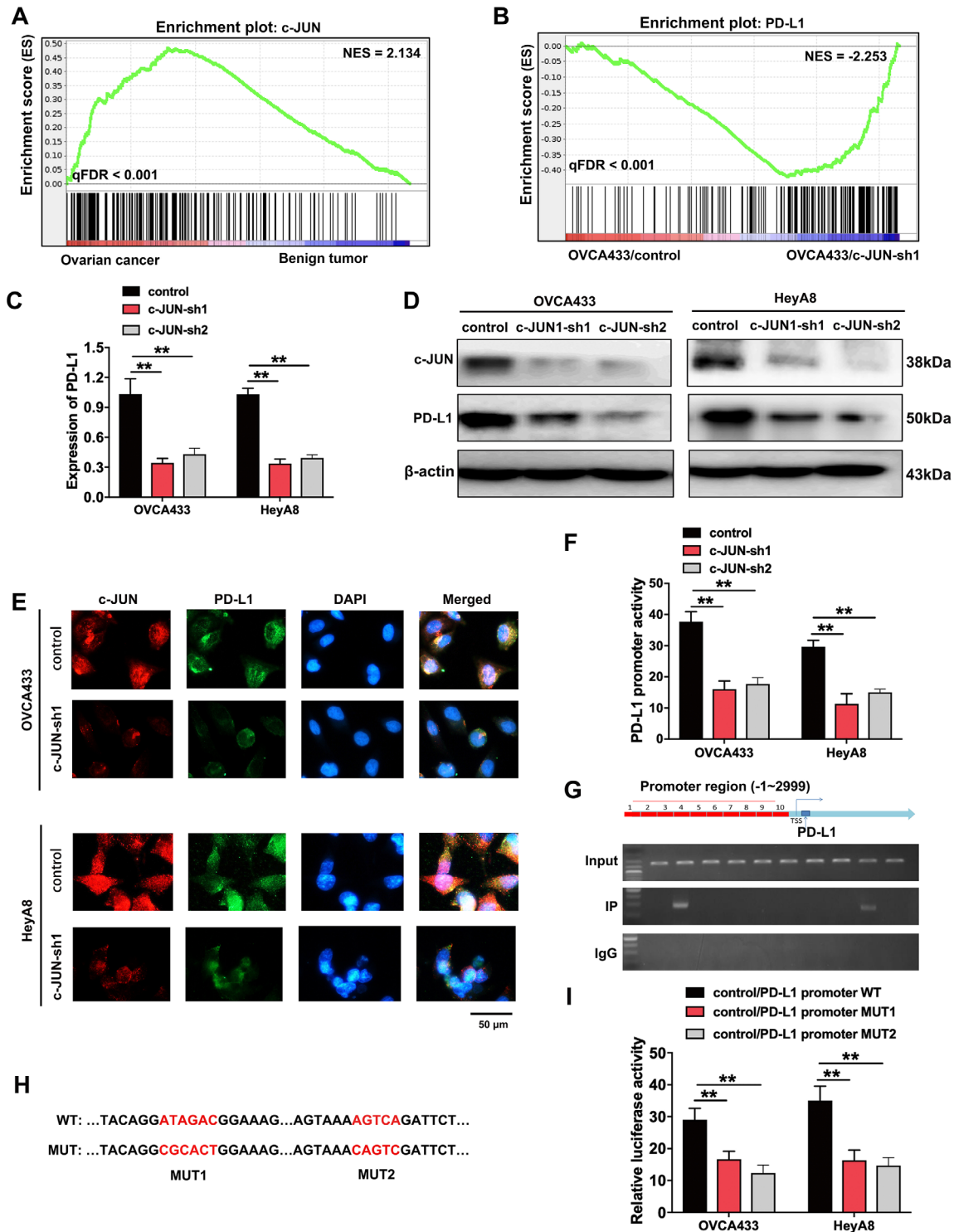


FIGURE 5 PD-L1 is the downstream targeting molecule of c-JUN, which is highly expressed in ovarian cancer tissues. (A) GSEA analysis was performed using ovarian cancer and benign tumor tissues. A gene signature was defined as a gene with significant expression changes. (B) GSEA analysis was performed using c-JUN-knockdown and control cells (OVCA433/c-JUN-sh1 and OVCA433/control). A gene signature was defined as a gene with significant expression changes. (C-D) qRT-PCR (C) and Western blotting (D) analysis of c-JUN and PD-L1. β -actin was used as a loading control. (E) Immunofluorescence assay demonstrates the relation of c-JUN and PD-L1. (F) PD-L1 promoter activity is affected by c-JUN silencing. (G) qRT-PCR results of ChIP analysis shows that c-JUN is bound to the PD-L1 gene promoter region. (H) The map of c-JUN-binding sites in the promoter region of PD-L1. (I) Luciferase reporter assay was used for the detection of c-JUN-mutant sites in the promoter region of PD-L1. $^{**}P < 0.01$. Abbreviations: PD-L1: programmed cell death-ligand 1; GSEA: gene set enrichment analysis; ES: enrichment score; NES: normalized enrichment score; FDR: false discovery rate; c-JUN-sh1/2: c-JUN short-hairpin RNA 1/2; qRT-PCR: quantitative real-time polymerase chain reaction; ChIP: chromatin immunoprecipitation; WT: wide type; MUT: mutant

by PD-L1 silencing, but drastically promoted by VEGFR2 overexpression with or without apatinib therapy (Figure 6A-E). Zebrafish development models were established for angiogenesis test *in vivo*. PD-L1 morpholino inhibited zebrafish angiogenesis, and this inhibition effect could be rescued by VEGFR2 overexpression (Figure 6F). VEGFA mRNA level was also reduced in PD-L1 morpholino group, which was rescued by the introduction of VEGFR2 cDNA (Figure 6G). Therefore, these data indicated that PD-L1 might induce angiogenesis and metastasis of ovarian cancer *in vivo*.

3.7 | Expression of PD-L1, c-JUN, VEGFR2, and VEGFA in ovarian cancer tissues

Firstly, through immunofluorescence, we verified that PD-L1 was highly expressed in metastatic ovarian cancer tissues than in primary cancer tissues (Figure 7A). Then, we performed IHC staining to examine the expression of c-JUN, VEGFR2, and VEGFA in 273 primary ovarian cancer tissues and 218 metastatic tissues. The results showed that c-JUN, VEGFR2, and VEGFA were highly expressed in metastatic ovarian cancer tissues compared with primary tumor samples ($P < 0.05$) (Figure 7B-C). The relative mRNA expression levels of metastasis-associated proteins such as AKT1, FAK, and N-cadherin were increased, and the level of E-cadherin expression was decreased in the metastatic ovarian cancer tissues compared with that in the primary tissues (Figure 7D). We demonstrated that PD-L1 and vascular endothelial cell-specific marker CD31 were highly expressed in metastatic ovarian cancer tissues and PD-L1 was bounded to CD31 by immunofluorescence (Figure 7E). Finally, we identified the c-JUN/PD-L1/VEGFR2 signaling axis in ovarian cancer (Figure 7F).

4 | DISCUSSION

In this study, we demonstrated that PD-L1 promoted the angiogenesis and metastasis of ovarian cancer by participating in the c-JUN/VEGFR2 signaling axis. Specifically, the PD-L1 inhibitor durvalumab combined with the antiangiogenic drug, apatinib, enhanced the effect of antiangiogenesis, which may be a new potential therapeutic approach for ovarian cancer.

Although some previous studies had disclosed the intrinsic role of PD-L1 in the promotion of the epithelial-to-mesenchymal transition (EMT) process and metastasis of cancer cells [28–30], the present study found new evidence for clarifying the molecular mechanism underlying these metastasis-driving events caused by PD-L1. For example, members of the integrin family, such as ITGB4

and ITGB6, were identified to directly interact with PD-L1 as its receptor, which further activated the downstream signaling pathway. However, our findings revealed that PD-L1 could bind to VEGFR2 and triggered signal transduction in ovarian cancer cells, activating the FAK/AKT pathway and enhancing cell migration and invasion. Meanwhile, the PD-L1/VEGFR2/FAK axis regulated the biological process of angiogenesis. Although other studies clarified the molecular mechanisms of ovarian cancer angiogenesis and metastasis [31, 32], the present study demonstrated that PD-L1 could act upon VEGFR2, a membrane receptor, to induce ovarian cancer cell angiogenesis and metastasis.

Cisplatin-based chemotherapy is an important adjuvant treatment for ovarian cancer. However, cisplatin resistance remains a critical event for ovarian cancer patients. Recent studies have concluded that PD-L1 inhibitors could exert an inhibitory effect on cell growth and proliferation in various cancer cells [33]. Currently, combined treatment modalities that target angiogenesis pathways hold promise for the treatment of chemoresistant cancer [10]. Accumulating evidence suggests that inhibition of angiogenesis enhances drug-induced apoptosis in a number of cancers [34, 35]. Our data also showed that the use of PD-L1 inhibitor in combination with VEGFR2 blockade could enhance the therapeutic effect of anti-angiogenesis targeting drugs, which can be used as new therapeutic approach for ovarian cancer patients.

c-JUN is an important member of activator protein-1, a kind of key transcription factor that participates in several important cellular processes such as cell survival proliferation and differentiation [36–38]. For example, the FAM83A/PI3K/AKT/c-JUN positive-feedback loop was proved to promote hepatocellular carcinoma migration, invasion, and metastasis by activating the EMT signaling pathway [39]. LINC00116 regulates tumorigenesis via the miR-106a/c-Jun axis in cervical cancer [40]. Here, we also showed that c-JUN could enhance the promoter activity of PD-L1 and promote PD-L1 transcription and expression, which partly illustrated the reason why the expression level of PD-L1 was increased in ovarian cancer.

By performing IHC staining assay with primary and metastatic ovarian cancer tissues and survival analysis, we further proved that PD-L1 could be regarded as a prognostic risk factor and induce ovarian cancer progression and metastasis. Previous studies have reported similar results in other types of cancer, such as head and neck cancer [41], colorectal cancer [42], endometrial cancer [43], and clear cell renal cell carcinoma [44]. PD-L1 was also found to play a vital role as a poor prognosis predictor in patients with biliary tract cancer [45]. These results further supported that PD-L1 could be considered as a potential therapeutic target in various cancers including ovarian cancer.

There remains some limitations. For example, PD-L1 could regulate glycolysis and the expression of

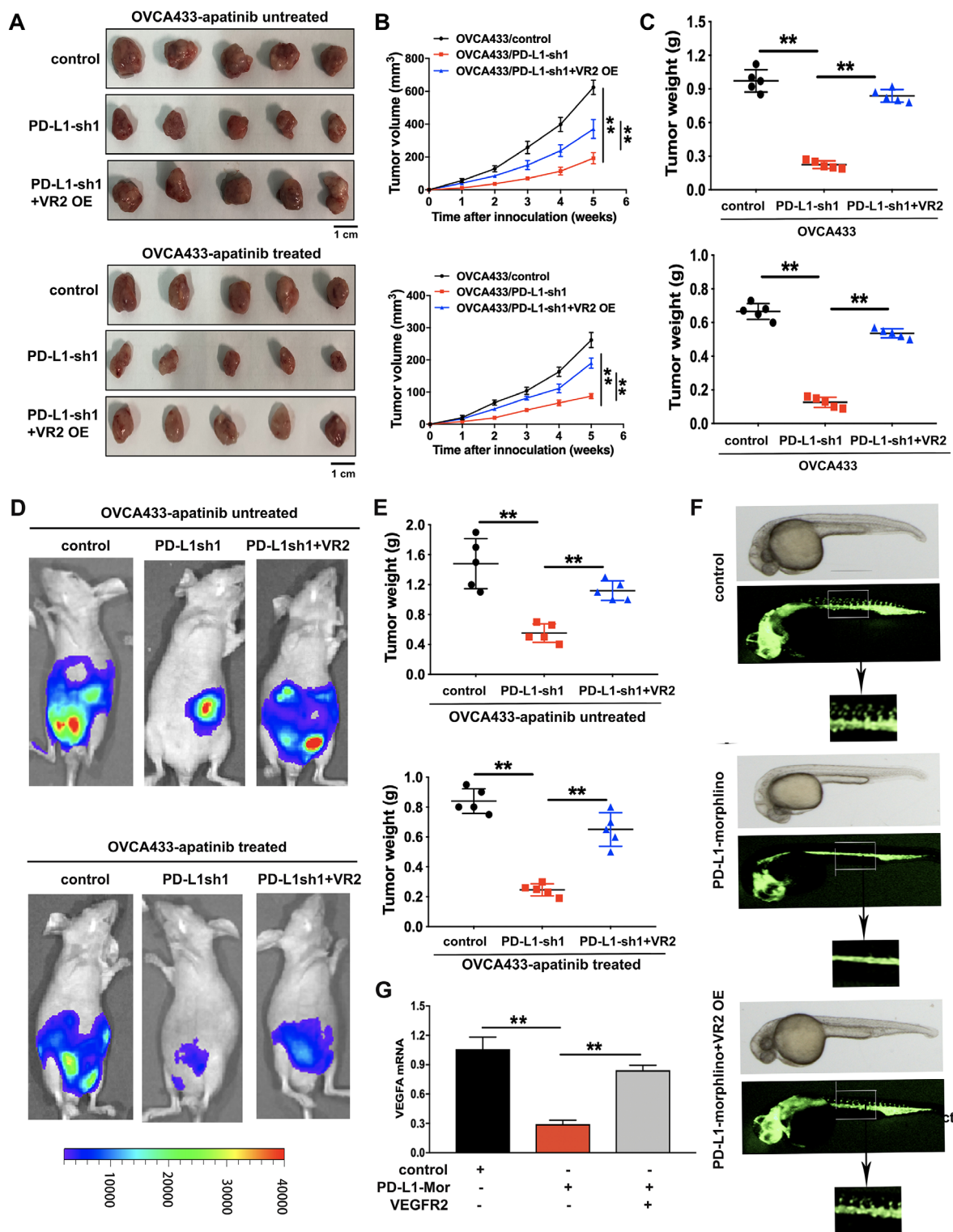
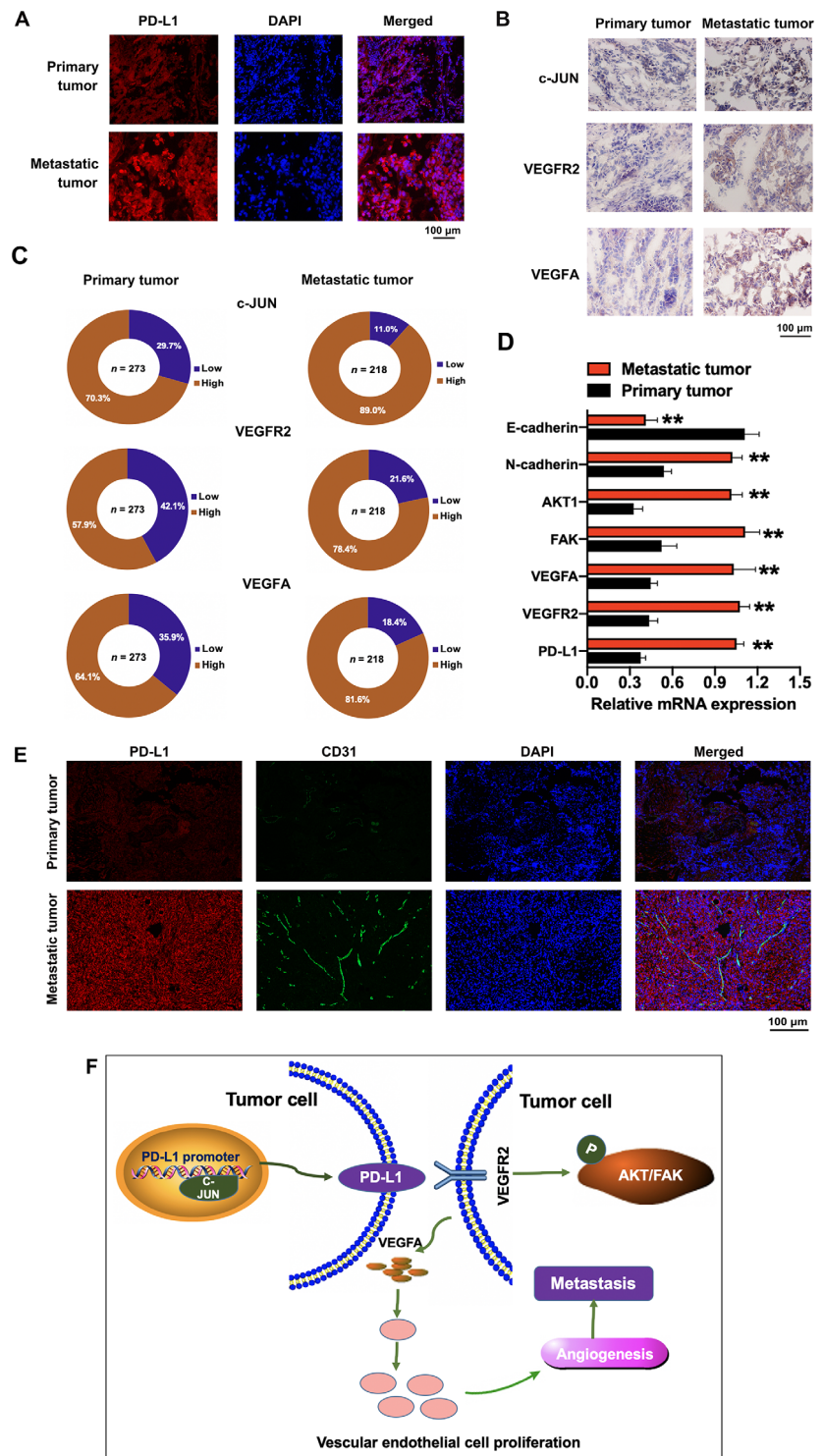


FIGURE 6 The effects of PD-L1 knockdown and VEGFR2 overexpression on the progression and angiogenesis of ovarian cancer *in vivo*. (A) Representative images of subcutaneous xenograft tumors formed by OVCA433/control, OVCA433/PD-L1-sh1, and OVCA433/PD-L1-sh1 + VEGFR2 overexpression (VR2 OE) cells in nude mice with or without apatinib treatment. (B) Growth curve of the xenograft tumors in mice with or without apatinib treatment. (C) The average tumor weight of nude mice with or without apatinib treatment. (D) Representative images of intraperitoneal xenograft tumors in nude mice with or without apatinib treatment. (E) The average weight of intraperitoneal xenograft tumors in nude mice. (F) Zebrafish model. Zebrafish embryos were injected with PD-L1 morpholino or VEGFR2 cDNA recombinant plasmid. (G) The mRNA expression levels of VEGFA assessed by qRT-PCR assay in zebrafish model. $^{**}P < 0.01$. Abbreviations: PD-L1: programmed cell death-ligand 1; PD-L1-sh1/2: PD-L1 short-hairpin RNA 1/2; VR2-OE: vascular endothelial growth factor receptor-2 overexpression; PD-L1-Mor: PD-L1 morpholino; qRT-PCR: quantitative real-time polymerase chain reaction

FIGURE 7 The PD-L1, c-JUN, VEGFR2, and VEGFA expression in primary and metastatic ovarian cancer tissues. (A) Immunofluorescence staining of PD-L1 in primary and metastatic ovarian cancer tissues. (B) Immunohistochemical staining of c-JUN, VEGFR2, and VEGFA in primary and metastatic ovarian cancer tissues. (C) The statistical results of the immunohistochemical staining of c-JUN, VEGFR2, and VEGFA. (D) The mRNA expression levels of genes associated with cell migration and angiogenesis were tested by qRT-PCR assay. (E) Immunofluorescence staining of PD-L1 and vascular endothelial cell-specific marker CD31 in primary and metastatic ovarian cancer tissues. (F) Schematic model showing the role of the c-JUN/PD-L1/VEGFR2 signaling axis in the regulation of angiogenesis. Abbreviations: PD-L1: programmed cell death-ligand 1; DAPI: 4',6-diamidino-2-phenylindole; qRT-PCR: quantitative real-time polymerase chain reaction; AKT1: protein kinase B; FAK: focal adhesion kinase; VEGFA: vascular endothelial growth factor A; VEGFR2: vascular endothelial growth factor receptor-2



glycolysis associated enzymes, but the mechanism remains not well known. In addition, further studies are required to deepen our understanding of the roles of PD-L1 in regulating metastasis-associated molecules during ovarian cancer progression. Clinical verifications of the combination of PD-L1 inhibitor and VEGFR2 blockade in ovarian cancer therapy are still needed.

5 | CONCLUSIONS

c-JUN is required for the PD-L1 expression, and PD-L1 could further activate the VEGFR2/AKT signaling pathway to enhance angiogenesis and invasion of ovarian cancer. The interaction between VEGFR2 and PD-L1 may be a target of more effective combination therapies.

DECLARATIONS

ETHICS APPROVAL AND CONSENT TO PARTICIPATE

This study was approved by the Ethics committee of Fudan University Shanghai Cancer Center. Each participant signed informed consent before participating in this study. All the authors approved the publication.

AUTHORS' CONTRIBUTIONS

XC, HZS, ZLW and LFX conceived and coordinated the project. YFY, ZLW, HZS, and YW performed most of the experiments and wrote the manuscript. HYZ and HRL performed *in vivo* studies. MDX, XC and ZHQ performed the immunohistochemistry, Western blotting, and immunofluorescence assays. All authors read and approved the final manuscript.

ACKNOWLEDGEMENTS

This work was supported by the National Natural Science Foundation of China (81502235, 81872117, and 82003053), Traditional Chinese Medicine Research Fund of Shanghai Municipal Commission of Health and Family Planning (WS-ZY1201), and a project supported by the Shanghai Municipal Health Commission (20194Y0039).

CONFLICTS OF INTERESTS

The authors declare no potential conflicts of interest.

AVAILABILITY OF DATA AND MATERIALS

The data that support the findings of this study are available from the corresponding author upon reasonable request.

ORCID

Ziliang Wang  <https://orcid.org/0000-0002-2702-5887>

REFERENCES

1. Siegel RL, Miller KD, Jemal A. Cancer statistics, 2019. *CA Cancer J Clin*. 2019;69:7-34.
2. Lian XY, Zhang H, Liu Q, Lu X, Zhou P, He SQ, et al. Ovarian cancer-excreted exosomal miR-199a-5p suppresses tumor metastasis by targeting hypoxia-inducible factor-2alpha in hypoxia microenvironment. *Cancer Commun (Lond)*. 2020; 40:380-5.
3. Ledermann JA, Raja FA, Fotopoulou C, Gonzalez-Martin A, Colombo N, Sessa C, et al. Newly diagnosed and relapsed epithelial ovarian carcinoma: ESMO Clinical Practice Guidelines for diagnosis, treatment and follow-up. *Ann Oncol*. 2018;29:iv259.
4. Topalian SL, Weiner GJ, Pardoll DM. Cancer immunotherapy comes of age. *J Clin Oncol*. 2011;29:4828-36.
5. Dong H, Strome SE, Salomao DR, Tamura H, Hirano F, Flies DB, et al. Tumor-associated B7-H1 promotes T-cell apoptosis: a potential mechanism of immune evasion. *Nat Med*. 2002;8:793-800.
6. Webb JR, Milne K, Kroeger DR, Nelson BH. PD-L1 expression is associated with tumor-infiltrating T cells and favorable prognosis in high-grade serous ovarian cancer. *Gynecol Oncol*. 2016;141:293-302.
7. Tothill RW, Tinker AV, George J, Brown R, Fox SB, Lade S, et al. Novel molecular subtypes of serous and endometrioid ovarian cancer linked to clinical outcome. *Clin Cancer Res*. 2008;14:5198-208.
8. Disis ML, Taylor MH, Kelly K, Beck JT, Gordon M, Moore KM, et al. Efficacy and Safety of Avelumab for Patients With Recurrent or Refractory Ovarian Cancer: Phase 1b Results From the JAVELIN Solid Tumor Trial. *JAMA oncol*. 2019;5:393-401.
9. Hamanishi J, Mandai M, Ikeda T, Minami M, Kawaguchi A, Murayama T, et al. Safety and Antitumor Activity of Anti-PD-1 Antibody, Nivolumab, in Patients With Platinum-Resistant Ovarian Cancer. *J Clin Oncol*. 2015;33:4015-22.
10. Hodi FS, O'Day SJ, McDermott DF, Weber RW, Sosman JA, Haanen JB, et al. Improved survival with ipilimumab in patients with metastatic melanoma. *N Engl J Med*. 2010;363:711-23.
11. Robert C, Long GV, Brady B, Dutriaux C, Maio M, Mortier L, et al. Nivolumab in previously untreated melanoma without BRAF mutation. *N Engl J Med*. 2015;372:320-30.
12. Chen W, Li Z, Zheng Z, Wu X. Efficacy and safety of low-dose apatinib in ovarian cancer patients with platinum-resistance or platinum-refractoriness: A single-center retrospective study. *Cancer Med*. 2020.
13. Huang Q, Chu C, Tang J, Dai Z. Efficacy and safety of apatinib combined with etoposide in patients with recurrent platinum-resistant epithelial ovarian cancer: a retrospective study. *J Cancer*. 2020; 11: 5353-8.
14. Rosenberg JE, Hoffman-Censits J, Powles T, van der Heijden MS, Balar AV, Necchi A, et al. Atezolizumab in patients with locally advanced and metastatic urothelial carcinoma who have progressed following treatment with platinum-based chemotherapy: a single-arm, multicentre, phase 2 trial. *Lancet*. 2016;387:1909-20.
15. Wang S, Li J, Xie J, Liu F, Duan Y, Wu Y, et al. Programmed death ligand 1 promotes lymph node metastasis and glucose metabolism in cervical cancer by activating integrin beta4/SNAI1/SIRT3 signaling pathway. *Oncogene*. 2018;37:4164-80.
16. Cao D, Qi Z, Pang Y, Li H, Xie H, Wu J, et al. Retinoic Acid-Related Orphan Receptor C Regulates Proliferation, Glycolysis, and Chemoresistance via the PD-L1/ITGB6/STAT3 Signaling Axis in Bladder Cancer. *Cancer Research*. 2019;79:2604-18.
17. Zhao R, Song Y, Wang Y, Huang Y, Li Z, Cui Y, et al. PD-1/PD-L1 blockade rescue exhausted CD8+ T cells in gastrointestinal stromal tumours via the PI3K/Akt/mTOR signalling pathway. *Cell Prolif*. 2019;52:e12571.
18. Gadducci A, Lanfredini N, Sergiampietri C. Antiangiogenic agents in gynecological cancer: State of art and perspectives of clinical research. *Crit Rev Oncol Hematol*. 2015;96:113-28.
19. Cereda V, Formica V, Roselli M. Issues and promises of bevacizumab in prostate cancer treatment. *Expert Opin Biol Ther*. 2018;18:707-17.

20. Haunschild CE, Tewari KS. Bevacizumab use in the frontline, maintenance and recurrent settings for ovarian cancer. *Future oncol*. 2019.
21. Burger RA, Brady MF, Bookman MA, Fleming GF, Monk BJ, Huang H, et al. Incorporation of bevacizumab in the primary treatment of ovarian cancer. *The New England journal of medicine*. 2011;365:2473-83.
22. Perren TJ, Swart AM, Pfisterer J, Ledermann JA, Pujade-Lauraine E, Kristensen G, et al. A phase 3 trial of bevacizumab in ovarian cancer. *N Engl J Med*. 2011;365:2484-96.
23. Aghajanian C, Blank SV, Goff BA, Judson PL, Teneriello MG, Husain A, et al. OCEANS: a randomized, double-blind, placebo-controlled phase III trial of chemotherapy with or without bevacizumab in patients with platinum-sensitive recurrent epithelial ovarian, primary peritoneal, or fallopian tube cancer. *J Clin Oncol*. 2012;30:2039-45.
24. Pujade-Lauraine E, Hilpert F, Weber B, Reuss A, Poveda A, Kristensen G, et al. Bevacizumab combined with chemotherapy for platinum-resistant recurrent ovarian cancer: The AURELIA open-label randomized phase III trial. *J Clin Oncol*. 2014;32:1302-8.
25. Coleman RL, Brady MF, Herzog TJ, Sabbatini P, Armstrong DK, Walker JL, et al. Bevacizumab and paclitaxel-carboplatin chemotherapy and secondary cytoreduction in recurrent, platinum-sensitive ovarian cancer (NRG Oncology/Gynecologic Oncology Group study GOG-0213): a multicentre, open-label, randomised, phase 3 trial. *Lancet Oncol*. 2017;18:779-91.
26. Gao H, Zhang J, Ren X. PD-L1 regulates tumorigenesis and autophagy of ovarian cancer by activating mTORC signaling. *Biosci Rep*. 2019; 39.
27. Abiko K, Matsumura N, Hamanishi J, Horikawa N, Murakami R, Yamaguchi K et al. IFN-gamma from lymphocytes induces PD-L1 expression and promotes progression of ovarian cancer. *Br J Cancer*. 2015; 112: 1501-9.
28. Chen L, Cheng X, Tu W, Qi Z, Li H, Liu F, et al. Apatinib inhibits glycolysis by suppressing the VEGFR2/AKT1/SOX5/GLUT4 signaling pathway in ovarian cancer cells. *Cell oncol*. 2019;42:679-90.
29. Welte J, Loges S, Dimmeler S, Carmeliet P. Recent molecular discoveries in angiogenesis and antiangiogenic therapies in cancer. *J Clin Invest*. 2013;123:3190-200.
30. Liu C, Peng X, Li Y, Liu S, Hou R, Zhang Y, et al. Positive feedback loop of FAM83A/PI3K/AKT/c-Jun induces migration, invasion and metastasis in hepatocellular carcinoma. *Biomed Pharmacother*. 2019;123:109780.
31. Chen J, Li X, Yang L, Li M, Zhang Y, Zhang J. CircASH2L Promotes Ovarian Cancer Tumorigenesis, Angiogenesis, and Lymphangiogenesis by Regulating the miR-665/VEGFA Axis as a Competing Endogenous RNA. *Front Cell Dev Biol*. 2020; 8:595585.
32. Zhu W, Liu C, Lu T, Zhang Y, Zhang S, Chen Q et al. Knockout of EGFL6 by CRISPR/Cas9 Mediated Inhibition of Tumor Angiogenesis in Ovarian Cancer. *Front Oncol*. 2020; 10: 1451.
33. Gao Q, Wang XY, Qiu SJ, Yamato I, Sho M, Nakajima Y, et al. Overexpression of PD-L1 significantly associates with tumor aggressiveness and postoperative recurrence in human hepatocellular carcinoma. *Clin Cancer Res*. 2009;15:971-9.
34. Cao Y, Zhang L, Kamimura Y, Ritprajak P, Hashiguchi M, Hirose S, et al. B7-H1 overexpression regulates epithelial-mesenchymal transition and accelerates carcinogenesis in skin. *Cancer Research*. 2011;71:1235-43.
35. Wang Y, Wang H, Zhao Q, Xia Y, Hu X, Guo J. PD-L1 induces epithelial-to-mesenchymal transition via activating SREBP-1c in renal cell carcinoma. *Med oncol*. 2015;32:212.
36. Zhang L, Chen Y, Li F, Bao L, Liu W. Atezolizumab and Bevacizumab Attenuate Cisplatin Resistant Ovarian Cancer Cells Progression Synergistically via Suppressing Epithelial-Mesenchymal Transition. *Front Immunol*. 2019;10:867.
37. Schiefer AI, Vesely P, Hassler MR, Egger G, Kenner L. The role of AP-1 and epigenetics in ALCL. *Front Biosci*. 2015;7:226-35.
38. Garces de Los Fayos Alonso I, Liang HC, Turner SD, Lagger S, Merkel O, Kenner L. The Role of Activator Protein-1 (AP-1) Family Members in CD30-Positive Lymphomas. *Cancers*. 2018;10.
39. Tewari D, Nabavi SF, Nabavi SM, Surenda A, Farooqi AA, Atanasov AG, et al. Targeting activator protein 1 signaling pathway by bioactive natural agents: Possible therapeutic strategy for cancer prevention and intervention. *Pharmacol Res*. 2018;128:366-75.
40. Lai Y, Zhou B, Tan Q, Xu J, Wan T, Zhang L. LINC00116 enhances cervical cancer tumorigenesis through miR-106a/c-Jun pathway. *J Cell Biochem*. 2019.
41. Eichberger J, Schulz D, Pschendl K, Fiedler M, Reichert TE, Bauer RJ et al. PD-L1 Influences Cell Spreading, Migration and Invasion in Head and Neck Cancer Cells. *Int J Mol Sci*. 2020;21.
42. Wang S, Yuan B, Wang Y, Li M, Liu X, Cao J et al. Clinicopathological and prognostic significance of PD-L1 expression in colorectal cancer: a meta-analysis. *Int J Colorectal Dis*. 2020.
43. Lu L, Li Y, Luo R, Xu J, Feng J, Wang M. Prognostic and Clinicopathological Role of PD-L1 in Endometrial Cancer: A Meta-Analysis. *Front Oncol*. 2020;10:632.
44. Stenzel PJ, Schindeldecker M, Tagscherer KE, Foersch S, Herpel E, Hohenfellner M, et al. Prognostic and Predictive Value of Tumor-infiltrating Leukocytes and of Immune Checkpoint Molecules PD1 and PDL1 in Clear Cell Renal Cell Carcinoma. *Transl oncol*. 2019;13:336-45.
45. Lei C, Peng X, Gong X, Fan Y, Wu S, Liu N, et al. Prognostic role of programmed death-ligand 1 expression in patients with biliary tract cancer: a meta-analysis. *Aging*. 2019;11:12568-80.

SUPPORTING INFORMATION

Additional supporting information may be found online in the Supporting Information section at the end of the article.

How to cite this article: Yang Y, Xia L, Wu Y, Zhou H, Chen X, Li H, et al. Programmed death ligand-1 regulates angiogenesis and metastasis by participating in the c-JUN/VEGFR2 signaling axis in ovarian cancer. *Cancer Commun*. 2021;1–17.
<https://doi.org/10.1002/cac2.12157>